

# Radical concentrations in free radical copolymerization of MMA/EGDMA

S. Zhu, Y. Tian and A. E. Hamielec\*

*Institute for Polymer Production Technology, Department of Chemical Engineering, McMaster University, Hamilton, Ontario, Canada L8S 4L7*

and D. R. Eaton

*Department of Chemistry, McMaster University, Hamilton, Ontario, Canada L8S 4L7*

*(Received 27 December 1988; revised 19 April 1989; accepted 21 April 1989)*

Radical concentration histories for the bulk free radical copolymerization of methyl methacrylate (MMA) and ethylene glycol dimethacrylate (EGDMA) initiated with 0.3 wt% 2,2'-azobis(2-methyl-propionitrile) (AIBN) at 70°C over the entire composition range were measured with an on-line electron spin resonance spectrometer. Radical concentrations of  $10^{-7}$ – $10^{-3}$  mol l<sup>-1</sup> were observed. At high EGDMA levels, the radical concentration increases monotonously from the onset of polymerization. Even in the glassy state, the radical concentrations continue to increase significantly. Once high concentrations of radicals which are chemically bound to the crosslinked network form, they are stable to temperature increases above the glass transition temperature. These stable radicals can propagate with a newly added monomer to the swollen gel. For low EGDMA levels (<25 wt%) there exist four stages of radical concentration change with reaction time (monomer conversion): (1) the radical concentration remains relatively constant for low monomer conversions; (2) at some intermediate conversion there is a dramatic rise; (3) after reaching a peak concentration there is a small decrease; (4) the concentration then increases gradually and levels off. The dramatic rise in the second stage is in agreement with the hypothesis that the autoacceleration of reaction rate in a free radical polymerization is due to an increase in the radical concentration. An analysis of the radical concentration rise rates reveals that the use of the quasi-stationary state hypothesis (QSSH) at high levels of crosslinking is not valid. These radical concentration measurements coupled with the corresponding conversion rate data give a direct estimate of the propagation constant ( $K_p$ ). The propagation constant was found to fall slightly at low conversions, but to fall dramatically at some high conversion where the conversion rate approaches zero. This explains why the polymerization rate of a bulk free radical polymerization run at  $T < T_{sp}$  (the glass transition temperature of the polymer) falls to almost zero even though appreciable monomer and initiator still exist in the reacting mass. The fall in  $K_p$  is in turn due to a radical trapping effect, i.e. the radical centres are surrounded by a solid environment consisting of polymeric segments. Using the assumption that bimolecular termination at high conversions is controlled by 'propagation diffusion', with  $K_t \propto K_p[M]$ , the initiation efficiency ( $f$ ) and the termination rate constant ( $K_t$ ) were also calculated from the data. The initiation efficiency was found to fall almost simultaneously with the propagation rate constant.

(Keywords: free radicals; electron spin resonance; crosslinking; radical trapping; copolymerization; methyl methacrylate; ethylene glycol dimethacrylate)

## INTRODUCTION

Free radical polymerization with crosslinking has been receiving more attention recently due to its potential for development of new polymer products, such as thermosetting moulding compounds, superabsorbents, coatings and ion exchange resins. Although some successes have been achieved in the manufacture of these materials, an understanding of the polymerization mechanisms and kinetics, which is essential for better control of the gel structure has not progressed far. One of the major unsolved problems is the lack of understanding of diffusion-controlled reactions. It is well accepted that many kinetic rate constants do not remain constant during such polymerizations, e.g. initiation efficiency, propagation rate constant and termination rate constant. These rate constants depend largely on the physical properties of the reacting system, which, in turn,

are strong functions of monomer conversion. The values of the rate constants may fall by orders of magnitude. In addition, the pendant double bonds and the radicals which are bound to the crosslinked polymer structure may experience shielding effects due to macromolecular chain conformation and concentration. Any serious attempt to model such polymerizations must account for these changes in rate constants with conversion. An objective of this work is to provide some basic measurements for the copolymerization of methyl methacrylate (MMA) and ethylene glycol dimethacrylate (EGDMA) to obtain a better understanding of diffusion-controlled reactions.

Although this model system has been studied for over four decades and some aspects of the kinetics have been investigated, such as gelation point<sup>1</sup>, glass transition temperature<sup>2</sup>, crosslink efficiency<sup>3</sup>, cyclization and reactivity of pendant double bond<sup>4,5</sup> and gel/sol fractions<sup>6</sup>, basic measurements which would help one to

\* To whom correspondence should be addressed

elucidate the mechanism of diffusion-controlled reactions are still lacking. An excellent study by Hayden *et al.*<sup>7</sup> gave estimates of the pseudo-propagation and termination rate constants using the rotating sector method. Unfortunately, this method is based on questionable assumptions such as the quasi-stationary state hypothesis (QSSH), the post-effect hypothesis and the assumption that the initiation efficiency does not change. A more direct method to estimate these parameters is to measure the radical concentration as a function of conversion. Early studies by Bamfort *et al.*<sup>8</sup> and Atherton *et al.*<sup>9</sup> provided measurements of the radical concentration versus reaction time using an electron spin resonance (e.s.r.) spectrometer with frozen samples to study radical trapping effects due to crosslinking. During the past three decades, modern e.s.r. techniques have advanced significantly. More recently, Kamachi *et al.*<sup>10</sup> and Bresler *et al.*<sup>11</sup> have measured the radical concentrations at initial stages of polymerization for some homopolymerization systems. Gilbert *et al.*<sup>12</sup> measured the propagation constant over the entire conversion range for the emulsion polymerization of MMA with frozen samples. Kamachi *et al.*<sup>10</sup> have pointed out difficulties when measuring radical concentrations in frozen samples by e.s.r.. Shen *et al.*<sup>13</sup> investigated the corresponding bulk polymerization of MMA in an e.s.r. cavity.

In this work, as a part of a systematic study of free radical polymerization with crosslinking<sup>6,14</sup>, we have measured radical concentrations during polymerization, in the e.s.r. cavity, of MMA/EGDMA over the entire composition range. Based on our measurements, coupled with corresponding conversion data<sup>6</sup>, and in light of the recent advances in the understanding of the mechanisms and kinetics of some homopolymerization systems<sup>15,16</sup>, we address questions of how the kinetic rate constants vary during the course of reaction, especially at very high conversions where the polymer/monomer forms a glass. In addition, we address the validity of QSSH at different conversions and crosslink densities.

## EXPERIMENTAL

MMA (Fisher Scientific) and EGDMA (Aldrich Chemicals) were purified as follows: washed with a 10 wt% aqueous KOH solution to remove inhibitor, washed with deionized water, dried successively with anhydrous sodium sulphate and 4 Å\* molecular sieves, and then distilled under reduced pressure using the middle fraction. 2,2'-Azobis(2-methyl-propionitrile) (AIBN) (Eastman Kodak) was recrystallized three times from absolute methanol.

Pyrex ampoules with 3 mm o.d. were used. The samples were degassed three times under a reduced pressure of  $10^{-4}$  mm Hg (15 mPa). Before the ampoules were sealed, they were filled with N<sub>2</sub> to reduce gas bubbles produced during reaction.

The prepared ampoule was then inserted into a TE110 cavity of a Bruker ER100D e.s.r. spectrometer. The polymerizations were implemented on-line to avoid the possible change of the radical concentration during quenching<sup>10</sup>. The reaction temperature was controlled with a high speed air bath at 70°C ( $\pm 0.5^\circ\text{C}$ ). The radical spectra were recorded frequently to follow the polymerization in detail.

An initiator concentration of 0.3 wt% AIBN was used. The nine weight fractions of EGDMA used were 0, 0.3, 1, 3, 5, 10, 15, 25 and 100 wt%. Five runs were done for each comonomer composition. Good reproducibility was achieved, as can be observed in the data plots shown later.

For low radical concentrations ( $< 10^{-6} \text{ mol l}^{-1}$ ), spectra were difficult to integrate and therefore the spectrum height ( $H$ ) and width ( $L_{pp}$ ) were carefully measured and corrected according to  $[R] \propto HL_{pp}^2$  (Reference 13). The absolute radical concentrations were calibrated with 2,2-diphenyl-1-picrylhydrazyl hydrate (DPPH) (Aldrich Chemicals) dissolved in MMA, covering a radical concentration range  $10^{-7}$ – $10^{-3} \text{ mol l}^{-1}$ , using the same type of ampoule.

The microwave power saturation behaviour of the MMA/EGDMA radical spectra were also studied.

## RESULTS AND DISCUSSION

Figures 1–3 show the radical concentration histories for the polymerizations with the nine EGDMA weight fractions. Characteristic features of these curves are as follows.

At low EGDMA levels (Figures 1 and 2), the polymerizations clearly show four stages in terms of the radical concentration behaviour versus reaction time. We consider the 1 wt% EGDMA run as an example. Coupled with corresponding conversion data<sup>6</sup>, the radical concentration measurements are plotted in Figure 4. As is shown, the radical concentration remains relatively

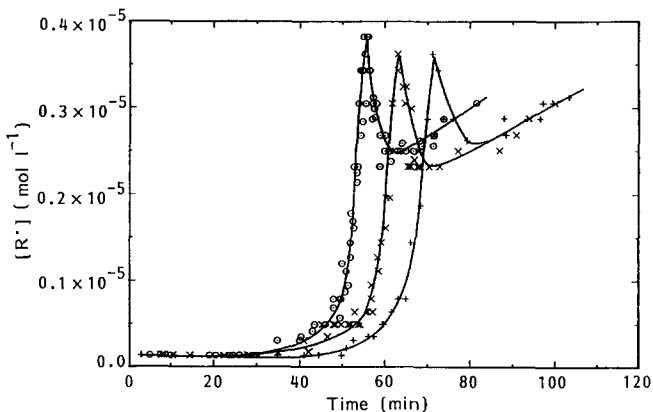


Figure 1 Radical concentrations of the polymerizations with 0 (+), 0.3 (x) and 1 (o) wt% EGDMA as a function of time.  $T = 70^\circ\text{C}$ ; AIBN, 0.3 wt%

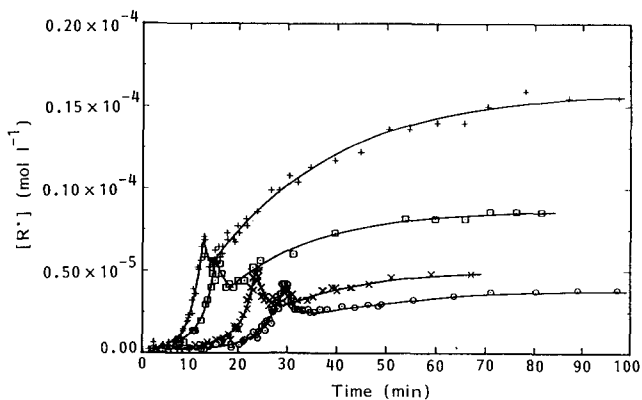
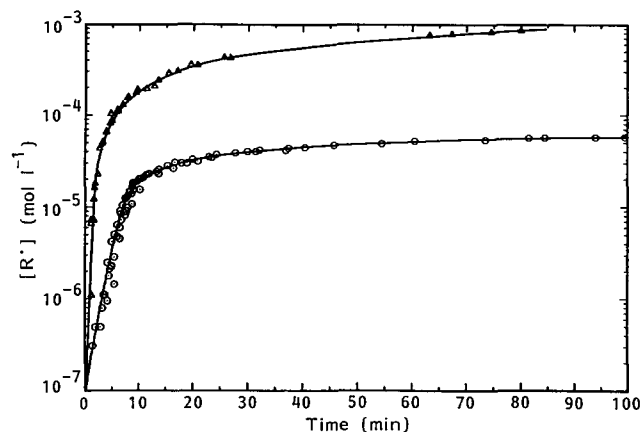
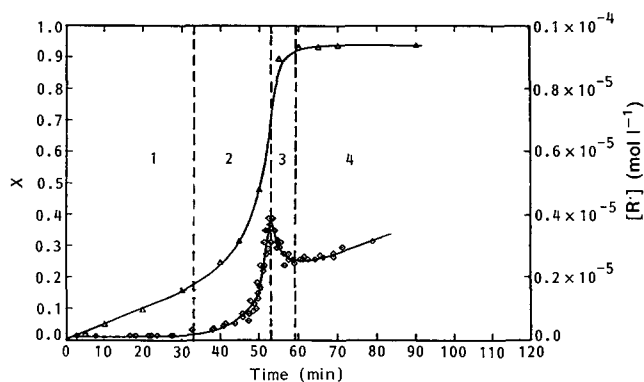


Figure 2 Radical concentrations of the polymerizations with 3 (o), 5 (x), 10 (□) and 15 (+) wt% EGDMA as a function of time.  $T = 70^\circ\text{C}$ ; AIBN, 0.3 wt%

\*1 Å =  $10^{-10}$  m



**Figure 3** Radical concentrations of the polymerizations with 25 (○) and 100 (△) wt% EDGMA as a function of time.  $T=70^{\circ}\text{C}$ ; AIBN, 0.3 wt%



**Figure 4** Radical concentration (◇) and monomer conversion (△) of the polymerization with 1 wt% EDGMA as a function of reaction time.  $T=70^{\circ}\text{C}$ ; AIBN, 0.3 wt%

constant initially (stage 1), where the QSSH is clearly valid. During this stage, the polymerization rate can be described by chemically controlled reactions.

In the second stage, both the radical concentration and the conversion rate show a synchronous rise. This verifies the hypothesis that the rapid autoacceleration in polymerization rate is due to a dramatic increase in radical concentration. An examination of the following equation:

$$d[R\cdot]/dt = 2fR_p - K_t[R\cdot]^2 \quad (1)$$

where  $R_p$  is the decomposition rate of the initiator,  $f$  is the initiation efficiency, the factor 2 accounts for the generation of two initiator radicals per molecule of initiator decomposed and  $K_t$  is the number average pseudo-termination rate constant<sup>20</sup>, which is defined as

$$K_t = K_{t11}\Phi_1\Phi_1 + 2K_{t12}\Phi_1\Phi_2 + K_{t22}\Phi_2\Phi_2$$

where subscripts 1,2 refer to monomers MMA and EDGMA, respectively and  $\Phi_i$  denotes the fraction of radical centres located on monomer  $i$ , reveals that this radical concentration rise is in turn due to a reduction in bimolecular termination rate of polymer radicals because the initiation efficiency  $f$  should not increase. Since the termination process involves two macroradicals diffusing together, such a reduction in rate may be caused by physical entanglement points of linear polymer chains in an MMA homopolymerization. This is often called the Trommsdorf or 'gel' effect (without gelation). For copolymerization with a divinyl monomer, this 'gel' effect

is coupled with the gelation effect, an additional hindrance to radical termination due to the chemically crosslinked structure (chemical entanglement points or crosslinks).

The diffusion-controlled termination in a free radical polymerization with crosslinking is even more complex. In fact, the macroradicals become highly branched before gelation. Such branched macroradicals probably experience limited translational diffusion in the reacting mass. Therefore, diffusion-controlled termination exists not only in the post-gelation period but also in the pre-gelation period. An experimental investigation of gelation with a 0.3 wt% EDGMA, for instance, gave a conversion at the gelation point ( $X_g$ ) of 0.24, while the autoacceleration starts at 0.15.

Note that, during the autoacceleration, the radical concentration rise rate  $d[R\cdot]/dt$  can be significant compared to the initiation rate ( $R_i$ ). We estimated the maximum  $(d[R\cdot]/dt)/R_i$  during autoacceleration using the experimental radical concentration versus time measurements. The initiation rate was estimated as follows:  $2fK_d[I] = 3.6 \times 10^{-5} \text{ mol l}^{-1} \text{ min}^{-1}$  initially, where the decomposition rate constant  $K_d = 1.83 \times 10^{-3} \text{ min}^{-1}$  for AIBN<sup>17</sup> at  $70^{\circ}\text{C}$ ;  $f_0 = 0.62$ ;  $[I]_0 = 0.0154 \text{ mol l}^{-1}$ . An evaluation of the validity of the QSSH is shown in Figure 5 for the different EDGMA weight fractions used. For high EDGMA concentrations,  $(d[R\cdot]/dt)/R_i$  reaches values as high as 0.6. For EDGMA concentrations  $\geq 10$  wt%, the QSSH is clearly invalid.

In stage 3, the radical concentration falls slightly after reaching a peak value. The peak radical concentrations for the different EDGMA weight fractions used are plotted in Figure 6. Such peaks correspond closely to maximum conversion rates. Thereafter, conversion rates start to fall. Note that this point may not be clearly seen from conversion/time data measured using some methods, such as the gravimetric method, which probably overestimates conversions at this stage due to the possible entrapment of monomer in glassy and highly crosslinked polymer and to residual polymerization during sample treatment. Temperature control may also be a problem when polymerization rates are very large.

Another interesting phenomenon, during stage 3, is the change in the e.s.r. spectra from 13-line to 9-line. Figure 7 gives an example of this transition. A 13-line spectrum indicates that the MMA radicals in the reacting mass are in a liquid environment, while a 9-line spectrum

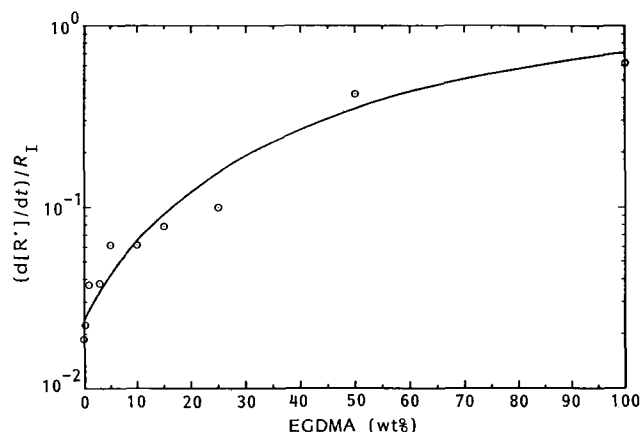


**Figure 5** Radical concentration rise rates during the autoaccelerations of the polymerizations with the different EDGMA weight fractions.  $T=70^{\circ}\text{C}$ ; AIBN, 0.3 wt%

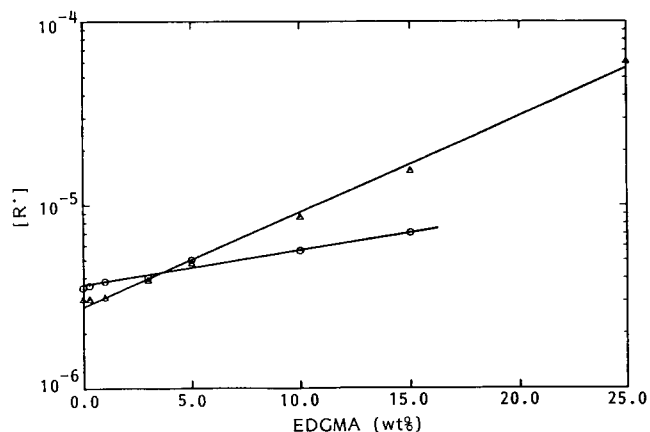


**Figure 6** Peak (○) and Final (△) radical concentrations of the polymerizations as a function of EGDMA weight fractions.  $T=70^{\circ}\text{C}$ ; AIBN, 0.3 wt%

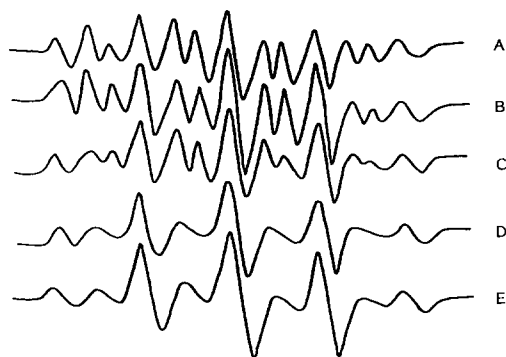


**Figure 7** Transition of 13-line spectra to 9-line spectra during the polymerization with 15 wt% EGDMA. Microwave frequency, 9.45 GHz; modulation frequency, 100 kHz; modulation amplitude, 3.2 Gpp (Gauss peak-to-peak); gain: A–B  $1 \times 10^6$ , C–E  $5 \times 10^5$ ; time: A, 9 min 15 s; B, 10 min 30 s; C, 12 min 20 s; D, 13 min 15 s; E, 20 min 30 s.  $T=70^{\circ}\text{C}$ ; AIBN, 0.3 wt%

is contributed from the EGDMA radicals and/or the MMA radicals in the solid state. These transitions in spectra suggest that the reacting system is approaching its glassy state.

Finally, in stage 4, the radical concentration increases again and then levels off. The final radical concentrations measured as a function of EGDMA weight fractions are also plotted in *Figure 6*. The final radical concentration is found to depend strongly on the weight fraction of EGDMA used. This suggests that the radicals bound on crosslinked polymer are not free to terminate or are trapped. A higher EGDMA level produces a tighter network structure, resulting in smaller bimolecular termination rates. Note also that the initiation rate is not zero even though the reacting mixture is in the glassy state. In fact, the radical concentration increases substantially during the final stage of polymerization (*Figures 1–3*).

The radical concentration measurements in the final stages of polymerization (stages 3, 4) are very informative and give one a better understanding of the polymerization mechanisms and kinetics at high conversions. The propagation constant  $K_p$  can be directly estimated using these radical concentration measurements coupled with the corresponding conversion/time data using the fundamental equation

$$dX/dt = K_p [R \cdot] (1 - X) \quad (2)$$

where  $K_p$  for binary copolymerization is given by the pseudo-propagation constant

$$K_p = K_{p11} \Phi_1 f_1 + K_{p12} \Phi_1 f_2 + K_{p21} \Phi_2 f_1 + K_{p22} \Phi_2 f_2$$

with  $K_{pij}$  the propagation constant for an  $i$ -type radical with monomer of type  $j$  and  $f_i = [M_i]/([M_1] + [M_2])$ . *Figure 8* shows the propagation constant for the homopolymerization of MMA using polymerization rate data after Li *et al.*<sup>6</sup> The propagation rate constant was found to remain relatively unchanged at low conversions, but to show a dramatic fall at the beginning of stage 3. This dramatic fall coincides with the reduction in conversion rate. Clearly, this great decrease in the propagation constant results in the extremely slow polymerization rate at high conversions. This is because most polymer radicals at this stage are effectively trapped in a glassy matrix and the diffusion rate of monomer limits the propagation rate.

In its glassy state, the reacting mass is probably heterogeneous. Therefore, two populations of radicals may exist. Those on crosslinked polymer and on large linear and branched polymer chains are shielded by a solid environment, which consists of polymeric segments and which limits monomer diffusion rate, and therefore lose reactivities. Those on relatively small chains (oligomeric radicals) may still be relatively mobile and create free volume. The monomer will also have higher diffusion coefficients in these more fluid regions. Accordingly, the propagation rate may be considered to be due to two separate rates as follows:

$$R_p = (K_{p,act} [R \cdot]_{act} + K_{p,ina} [R \cdot]_{ina}) [M] \quad (3)$$

where subscripts act and ina represent the active and the shielded radicals, respectively.  $K_{p,ina}$  is much smaller than  $K_{p,act}$ , while  $[R \cdot]_{ina}$  may be much higher than  $[R \cdot]_{act}$ . Therefore, the rate constants should be well defined in terms of the radical concentrations at this stage of polymerization, either the active or the global one (active + inactive).

Conversion/time and radical concentration/time data alone are known to be inadequate to estimate the changing termination rate constants and initiation efficiency. However, some aspects of the behaviour of  $K_t$  and  $f$  can be examined at high conversions. The termination rate at high conversions is thought to be controlled by 'propagation diffusion', i.e.

$$K_t = z K_p [M] \quad (4)$$

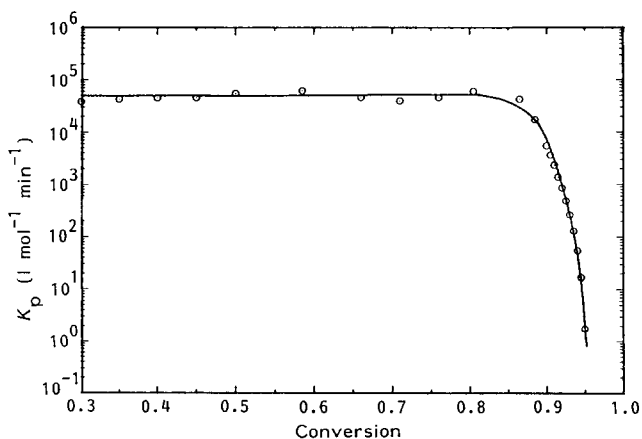


**Figure 8** Propagation rate constant behaviour of the polymerizations of MMA as a function of conversion.  $T=70^{\circ}\text{C}$ ; AIBN, 0.3 wt% (rate data after Li *et al.*<sup>6</sup>)

where  $z$  may be considered a constant over a small range of conversion<sup>18</sup>. Assume that the initiation efficiency  $f$  is equal to its initial value up to the peak radical concentration. At the peak, we have  $2fR_D = zK_p[M][R\cdot]^2$ . Therefore,  $z = 2fR_D/K_p[M][R\cdot]^2$  and can be calculated accordingly. Combining equations (1), (2) and (4) and using the radical concentration measurements with the corresponding conversion data, we estimated  $f$  and  $K_t$  ( $=zK_p[M]$ ). Figure 9 shows calculated values for 1 wt% EGDMA. It was found that  $f$  starts to fall a little earlier, but with a smaller rate, than  $K_p$  (in turn  $K_t$ ). It is this small time discrepancy that leads to the radical concentration decrease in stage 3. The discrepancy depends on the relative diffusion coefficients of the initiator radical and the monomer molecule and also the reaction conditions such as temperature. An experimental investigation of the homopolymerization of MMA initiated with dimethyl 2,2'-azodiisobutyrate (AIBME) at 60°C does not show such a peak<sup>13</sup>.

We believe that the initiation efficiency  $f$  must fall at high conversions. This fall, combined with the radical trapping concept, clearly explains why some bulk homopolymerizations ( $< T_{gp}$ ), MMA for instance, are extremely slow at high conversions while the corresponding emulsion polymerizations are not. In the latter polymerizations, initiator radicals are generated in the water phase, and diffuse into the monomer-polymer particles. Therefore, appreciable concentrations of radicals with short chains always exist in the polymer particles. These oligomeric radicals are still active (mobile), i.e. give a significant value for the first term in equation (3). In contrast, in a bulk polymerization, radicals are generated via initiator decomposition in the reacting mass. Due to the so-called 'cage effect', some initiator radicals recombine to form inert molecules. At high conversions, the initiator radicals find it difficult to migrate apart and most often recombine. Therefore, few active radicals exist in the reacting mass. Most of the radicals accumulated earlier have long chains, and are trapped. The discrepancy between the  $K_p$  values of the bulk and the emulsion polymerization is, in fact, due to the different active radical concentrations in the two processes.

A final point worth mentioning, concerning our experimental investigation, is that the polymer radicals obtained at the low EGDMA levels and at the final

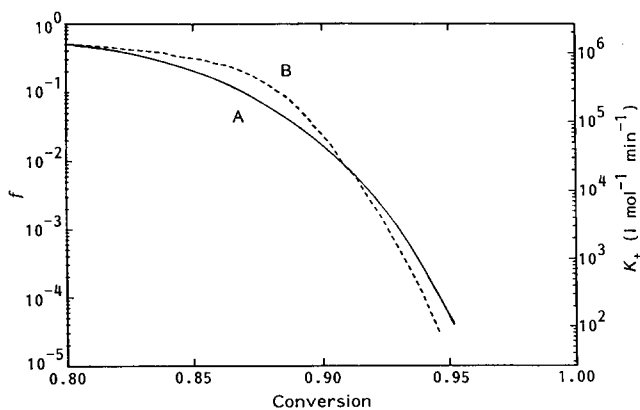


Figure 9 A, Initiation efficiency  $f$  and B, termination rate constant  $K_t$  at high conversions of the polymerization with 1 wt% EGDMA, calculated based on the assumption  $K_t \propto K_p[M]$ .  $T = 70^\circ\text{C}$ ; AIBN, 0.3 wt%

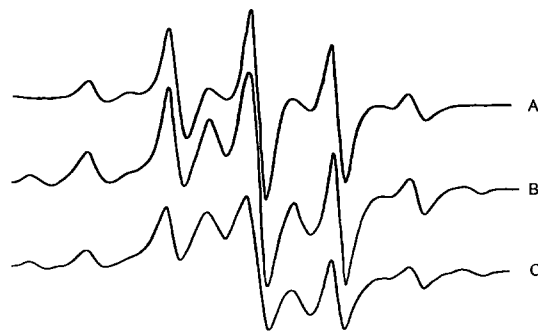


Figure 10 E.s.r. spectra of the EGDMA polymerization at final conversions measured at different temperatures; A, 70°C, polymerized for 100 min; B, 150°C, 10 min added; C, 150°C, 30 min added. E.s.r. conditions as in Figure 7. Gain: A,  $5 \times 10^4$ ; B, C,  $1.25 \times 10^5$ .  $T = 70^\circ\text{C}$ ; AIBN, 0.3 wt%



Figure 11 Change in the e.s.r. spectra from A, 50 wt% EGDMA, polymerized for 100 min, to B, reacted with the swelled styrene monomer for 10 h thereafter. Gain: A,  $5 \times 10^4$ ; B,  $5 \times 10^5$ . Other e.s.r. conditions as in Figure 7.  $T = 70^\circ\text{C}$ ; AIBN, 0.3 wt%

conversions are not stable at high temperatures, and their e.s.r. spectra disappear in minutes after the temperature is raised to  $> T_{gp}$ . On the other hand, the radicals bound to highly crosslinked polymers are quite stable. These radicals are hardly terminated even though the reaction temperature is raised to 150°C (according to Horie *et al.*<sup>19</sup>,  $T_{gp} = 141^\circ\text{C}$  for EGDMA homopolymer). Figure 10 gives an example of this radical stability. These highly concentrated, stable radicals may lead to some novel commercial materials, because they can be further reacted with other monomers added later in the polymerization. As a first attempt, we used a sample of 50 wt% EGDMA polymerized at 70°C for 100 min and then swelled the gel with styrene monomer. After degassing, the sample was polymerized again at 80°C for some time. As shown in Figure 11, the styrene e.s.r. signal was clearly detected. This signal comes from the styryl radicals grafted onto the crosslinked polymer.

#### ACKNOWLEDGEMENTS

Financial assistance from the Natural Sciences and Engineering Research Council of Canada, the Ontario Centre for Materials Research and the McMaster Institute for Polymer Production Technology (MIPPT) is appreciated.

#### REFERENCES

- 1 Walling, C. *J. Am. Chem. Soc.* 1945, **67**, 441
- 2 Loshaek, S. *J. Polym. Sci.* 1955, **15**, 391
- 3 Loshaek, S. and Fox, T. G. *J. Am. Chem. Soc.* 1953, **75**, 3544
- 4 Whitney, R. S. and Burchard, W. *Makromol. Chem.* 1980, **181**, 869

- 5 Landin, D. T. and Macosko, C. W. *Macromolecules* 1988, **21**, 846
- 6 Li, W.-H., Hamielec, A. E. and Crowe, C. M. *Polymer* 1989, **30**, 1513
- 7 Hayden, P. and Melville, H. W. *J. Polym. Sci.* 1960, **43**, 201, 215
- 8 Bamford, C. H., Jenkins, A. D., Symons, M. C. R. and Townsend, M. G. *J. Polym. Sci.* 1959, **34**, 181
- 9 Atherton, N. M., Melville, H. W. and Whiffen, D. H. *J. Polym. Sci.* 1959, **34**, 199
- 10 Kamachi, M. *Adv. Polym. Sci.* 1987, **82**, 207
- 11 Bresler, S. E., Kozbekov, E. N., Fomichev, V. N. and Shadrin, V. N. *Makromol. Chem.* 1974, **175**, 2875
- 12 Ballard, M. J., Gilbert, R. G., Napper, D. H., Pomery, P. J. and O'Donnell, J. H. *Macromolecules* 1984, **17**, 504
- 13 Shen, J., Tian, Y., Zeng, Y. and Qiu, Z. *Makromol. Chem., Rapid. Commun.* 1987, **8**, 615
- 14 Tobita, H. and Hamielec, A. E. *Macromolecules* 1989, **22**, 3098
- 15 Russell, G. T., Napper, D. H. and Gilbert, R. G. *Macromolecules* 1988, **21**, 2141
- 16 Tian, Y. *PhD Thesis* Jilin University, China, 1988
- 17 Tobolsky, A. V. and Baysal, B. *J. Polym. Sci.* 1953, **11**, 471
- 18 Stickler, M., Panke, D. and Hamielec, A. E. *J. Polym. Sci., Polym. Chem. Edn.* 1984, **22**, 2243
- 19 Horie, K., Otagawa, A., Muraoka, M. and Mita, I. *J. Polym. Sci., Polym. Chem. Edn.* 1975, **13**, 445
- 20 Zhu, S. and Hamielec, A. E. *Macromolecules* 1989, **22**, 3093